Empirical formula for over-barrier strong-field ionization

Qingbin Zhang, Pengfei Lan,* and Peixiang Lu

School of Physics and Key Laboratory of Fundamental Physical Quantities Measurement of Ministry of Education, Huazhong University of Science and Technology, Wuhan 430074, China

(Received 1 May 2014; published 13 October 2014)

A modified empirical ionization formula is proposed to extend Tong and Lin's ionization formula [X. M. Tong and C. D. Lin, J. Phys. B **38**, 2593 (2005)] to a laser field up to 4.5 times barrier-suppression strength (E_b) in the over-barrier regime. The validity of the formula is checked by solving the Schrödinger equation within the single-active-electron approximation with an excellent agreement. This modified empirical formula still keeps its simplicity and can calculate ionization rates in the deep over-barrier regime.

DOI: 10.1103/PhysRevA.90.043410 PACS number(s): 32.80.Fb, 32.80.Rm

I. INTRODUCTION

In strong-field physics, the ionization stands out as a fundament since it triggers the subsequent process. When the atomic or molecular gas is exposed to an intense femtosecond laser, an electron enters the continuum by ionization. Thereafter, the ionized electron can be accelerated away, recolliding with the ion either elastically or inelastically, with the interaction of an oscillated laser field. Moreover, the second electron may be triggered by the laser-driven recollision of the first electron with its parent ion or liberated by subsequent field induced ionization. These exciting phenomena are known as above threshold ionization [1], high-order harmonic generation [2], and nonsequential and sequential double ionization [3], and a great number of experimental as well as theoretical studies have been performed during the past decades.

To understand these phenomena, the first step is the accurate evaluation of the ionization rates on the laser intensities. Even though the quantum simulation based on the time-dependent or -independent Schrödinger equation can give an accuracy ionization rate, such a simulation is very time consuming for some applications. For instance, the evaluation of the phase matching of high harmonic generation (HHG) depends critically on the ionization of the macroscopic medium, and the calculations of ionization rates have to be carried out for thousands of laser peak intensities in order to include the nonuniform distribution inside a focused laser beam. At present, it is still a big challenge to simulate the phase matching of HHG by straightforwardly solving the Schrödinger equation. Actually an analytical ionization formula is highly desired in strong-field investigations, especially in the analysis of the experimental results, which will help us easily pick out the essential physical problems. The calculation of the ionization rate has been significantly simplified by introducing an analytical ionization formula with the Ammosov-Delone-Krainov (ADK) model [4] or Perelomov-Popov-Terent'ev model [5]. In the tunneling ionization regime, ADK theory agrees well with the quantum simulation, and therefore this formula has become a fundamental tool for strong-field physicists. Recently, O. I. Tolstikhin and coworkers further developed the ionization formula at the quantitative lever toward the strong field and molecule, based on weak-field asymptotic theory (WFAT). The region of applicability of WFAT has been extended to the barrier-suppression strength by introducing higher-order corrections and molecule by including the structure factor [6–11]. The WFAT ionization formula works better than ADK in the tunneling regime and has a nice physical interpretation behind the correction terms. However, in the over-barrier ionization regime, where the barrier of the Coulomb potential becomes suppressed by the electric field, the above-mentioned ionization formulas do not work. For example, it was clearly shown that the ADK model overestimates the ionization rate compared with the quantum simulation when $E > E_b$ [12]. Here $E_b = I_p^2/4/Z_c$, with I_p and Z_c being the ionization energy and charge of the ion under investigation, is defined as the barrier-suppression strength. To overcome this problem, Tong and Lin [13] proposed an empirical factor to draw up the ADK rate to the quantum simulation one, while maintaining the simplicity of the ADK formula. Even though the physical meaning of Tong and Lin's empirical factor is unknown, it still works well when the laser field reaches $2E_b$ and really simplifies the calculation of the ionization rate. Therefore it has been extensively employed in the analysis of experimental data [14–17].

On the other hand, the development of a femtosecond laser with higher intensity spanning from near infrared to midinfrared [18–23] has simulated the strong-field investigations on a broader set of problems; for example, a close-to-circular laser field with intensity reaching several petawatts has been used for timing the release for the double ionized electrons [14,24–26]. In these investigations, the applied laser intensity reaches 5×10^{15} W/cm^2, which corresponds to a field strength of $4.5E_b$ for Ar. For this reason, it is necessary to evaluate the performance of Tong and Lin's formula in a higher intensity regime. Does the accuracy depend on the laser intensity? If yes, what is the working range of this formula? Moreover, if a single-active-electron (SAE) potential is employed in [13], does the accuracy of Tong and Lin's formula depend on different SAE potentials? In this paper, Tong and Lin's formula is checked against the ionization rate obtained from the Schrödinger equation with different SAE potentials, and it is found that the ionization rate is underestimated by using Tong and Lin's formula if $E > 2E_b$. Finally a modified empirical analytical formula is proposed to correct this deviation, and it shows the formula works very well in the deep over-barrier regime.

*Corresponding author: pengfeilan@hust.edu.cn

TABLE I. Parameters of the SAE potential model adopted by Tong and Lin.

Target	Z_c	a_1	a_2	a_3	a_4	a_5	a_6
H	1.0	0.000	0.000	0.000	0.000	0.000	0.000
He	1.0	1.231	0.662	−1.325	1.236	−0.231	0.480
Ne	1.0	8.069	2.148	−3.570	1.986	0.931	0.602
Ar	1.0	16.039	2.007	−25.543	4.525	0.961	0.443
Xe	1.0	51.356	2.112	−99.927	3.737	1.644	0.431
Ne^+	2.0	8.043	2.715	0.506	0.982	−0.043	0.401
Ar^+	2.0	14.989	2.217	−23.606	4.585	1.011	0.551

TABLE II. Parameters of the GSZ potential model.

Target	Z	Z_c	H	d
He	2.0	1.0	0.674	0.381
Ne	10.0	1.0	2.219	0.751
Ar	18.0	1.0	3.469	0.997
Kr	36.0	1.0	5.507	1.055
Xe	54.0	1.0	6.805	1.175
Ne^+	10.0	2.0	1.426	0.485
Ar^+	18.0	2.0	3.098	0.835

TABLE III. Parameters of the Muller potential model.

Target	Z	Z_c	A	B	C
He	2.0	1.0	0.00	0.000	2.134
Ne	10.0	1.0	2.74	1.082	3.400
Ar	18.0	1.0	5.40	1.000	3.682
Ar^+	18.0	2.0	4.00	1.000	3.682

TABLE IV. Eigenenergies of several bound states of He.

State	GSZ	Muller	Tong-Lin	NIST
1*s*	–0.917 24	–0.903 37	–0.903 82	–0.903 95
2*s*	–0.158 33	–0.157 36	–0.160 01	–0.175 29
2*p*	–0.127 34	–0.127 98	–0.129 99	–0.123 87
3*s*	–0.064 64	–0.061 83	–0.062 33	–0.061 29
3*d*	–0.055 57	–0.053 99	–0.054 38	–0.055 64

TABLE V. Eigenenergies of several bound states of Ne.

State	GSZ	Muller	Tong-Lin	NIST
2*p*	–0.794 66	–0.798 92	–0.793 31	–0.792 81
3*s*	–0.180 82	–0.190 84	–0.196 54	–0.173 43
3*p*	–0.107 63	–0.111 08	–0.117 35	–0.117 02
4*s*	–0.069 51	–0.071 23	–0.070 51	–0.069 87

TABLE VI. Eigenenergies of several bound states of Ar.

State	GSZ	Muller	Tong-Lin	NIST
3*p*	–0.578 30	–0.580 52	–0.578 58	–0.579 40
4*s*	–0.151 29	–0.153 55	–0.164 59	–0.154 83
4*p*	–0.096 10	–0.096 99	–0.104 56	–0.091 07
3*d*	–0.063 44	–0.062 87	–0.070 11	–0.068 24

TABLE VII. Eigenenergies of several bound states of Ne^+.

State	GSZ	Muller	Tong-Lin	NIST
2*p*	–1.536 71		–1.505 22	–1.506 41
3*s*	–0.488 11		–0.504 83	–0.507 14
3*p*	–0.360 17		–0.371 85	–0.370 49
4*s*	–0.214 54		–0.219 61	–0.214 54
3*d*	–0.228 54		–0.236 16	–0.221 84

II. THEORETICAL MODEL AND RESULTS

A. SAE potential models

According to the ADK ionization theory, the ionization rate is expressed as (atomic units are used)

$$W_{\mathrm{ADK}}(E) = \frac{C_l^2}{2^{|m|}|m|!}\frac{(2l+1)(l+|m|)!}{2(l-|m|)!} \times \frac{1}{\kappa^{2Z_c/\kappa-1}}\left(\frac{2\kappa^3}{E}\right)^{2Z_c/\kappa-|m|-1}\exp(-2\kappa^3/3/E), \quad (1)$$

where l and m ($m = 0$ in our calculation) are the angular momentum and magnetic quantum numbers of the valence electrons, C_l is the coefficient that describes the electron wave function in the asymptotic region and its expression can be found in [27], and $\kappa = \sqrt{2I_p}$. For the electric field $E \to 0$ the theory of tunneling ionization can be summarized by an asymptotic expansion of the form

$$W_{\mathrm{WFAT}} = cE^b \exp^{-a/E}(1 + AElnE + BE + \ldots), \quad (2)$$

where the coefficients a, b, c, etc., do not depend on E and can be found in [9]. The dots indicate the existence of higher-order terms. This expansion applies in the interval $E < E_b$. Equation (1) is a special case of Eq. (2) with correction terms neglected.

To extend the ionization formula to the above barrier ionization regime, Tong and Lin proposed to modify the ADK formula using an empirical fitting factor α:

$$W_{\mathrm{TL}}(E) = \exp\left[-\alpha\left(Z_c^2/I_p\right)(E/\kappa^3)\right]W_{\mathrm{ADK}}(E). \quad (3)$$

To check the performance of the above formula, the static ionization rate is simulated by solving the Schrödinger equation with the complex scaling method. The Hamiltonian is

$$H = \left[-\frac{\nabla^2}{2} + V(r) + zE\right]. \quad (4)$$

By multiplying the coordinates with a complex factor $\exp(i\theta)$, the Hamiltonian becomes a non-Hermitian matrix which leads to complex eigenvalues. The real part of the eigenvalue stands

TABLE VIII. Eigenenergies of several bound states of Ar^+.

State	GSZ	Muller	Tong-Lin	NIST
3*p*	–1.020 93	–1.012 12	–1.014 94	–1.015 83
4*p*	–0.293 47	–0.297 82	–0.304 15	–0.293 64
4*s*	–0.390 62	–0.397 27	–0.403 06	–0.397 69
3*d*	–0.341 85	–0.329 15	–0.352 21	–0.363 48

TABLE IX. Half static ionization rate of Ar.

Field amplitude (intensity)	$\Gamma/2$: GSZ	$\Gamma/2$: Muller	$\Gamma/2$: Tong-Lin
0.053 29 (1.000×10^{14})	8.7871×10^{-6}	8.2616×10^{-6}	1.0464×10^{-5}
0.093 99 (3.111×10^{14})	2.6916×10^{-3}	2.6573×10^{-3}	3.3095×10^{-3}
0.121 77 (5.222×10^{14})	0.011 10	0.013 229	0.011 10
0.144 30 (7.333×10^{14})	0.021 66	0.021 782	0.025 03
0.163 76 (9.444×10^{14})	0.032 08	0.032 306	0.036 06
0.181 14 (1.156×10^{15})	0.041 43	0.041 682	0.045 43
0.196 99 (1.367×10^{15})	0.049 41	0.049 612	0.053 05
0.211 66 (1.578×10^{15})	0.056 07	0.056 152	0.059 17
0.225 37 (1.789×10^{15})	0.061 58	0.061 511	0.064 11
0.238 30 (2.000×10^{15})	0.066 17	0.0659 25	0.068 16
0.249 93 (2.200×10^{15})	0.069 84	0.069 433	0.071 37
0.267 76 (2.525×10^{15})	0.074 76	0.0741 13	0.075 68
0.284 47 (2.850×10^{15})	0.078 80	0.077 925	0.079 24
0.300 25 (3.175×10^{15})	0.082 20	0.081 178	0.082 30
0.315 24 (3.500×10^{15})	0.085 23	0.084 068	0.085 05

for the resonant energy and the imaginary part gives one-half of the ionization rate. In principle, the solution should be independent of the angle θ and we must find this special point where the resonant energy of the system will not change with it. By plotting the θ dependent eigenvalues in a complex plane [28], the stationary point is determined to be around $\theta = 0.4$, indicating that this is a reasonable angle for convergence studies. $V(r)$ in Eq. (4) denotes the SAE potential. Tong and Lin adopted the SAE potential model as shown below [13]:

$$V(r) = -\frac{Z_c + a_1 e^{-a_2 r} + a_3 r e^{-a_4 r} + a_5 e^{-a_6 r}}{r}, \qquad (5)$$

and then the parameters are shown in Table I for different atoms.

Other SAE potential models are also extensively used in strong-field physics [9,29]. One is proposed by Green, Sellin, and Zachor (GSZ) [30], which is expressed by

$$V(r) = -\frac{\frac{(Z-Z_c)}{H(e^{r/d}-1)+1} + Z_c}{r}. \qquad (6)$$

The other one is proposed by Muller [31], which has the form

$$V(r) = -\frac{Z_c + Ae^{-\mathrm{Br}} + (Z - Z_c - A)e^{-\mathrm{Cr}}}{r}. \qquad (7)$$

The corresponding parameters are shown in Tables II and III, respectively.

B. Comparison of the SAE potential models: eigenenergy of the bound states

First the eigenenergies of several bound states are calculated to compare the performance of these SAE potential models. The results are shown in Tables IV–VIII. We can see that the eigenenergies of the bound states obtained with these three models are consistent and also agree reasonably well with the values estimated from the atomic spectra given by NIST [32].

TABLE X. Half static ionization rate of Ar^+.

Field amplitude (intensity)	$\Gamma/2$: GSZ	$\Gamma/2$: Muller	$\Gamma/2$: Tong-Lin
0.075 36 (2.000×10^{14})	6.0344×10^{-8}	7.2791×10^{-8}	6.6251×10^{-8}
0.123 06 (5.333×10^{14})	2.8655×10^{-4}	3.8221×10^{-4}	3.7933×10^{-4}
0.156 87 (8.667×10^{14})	3.5719×10^{-3}	4.4861×10^{-3}	4.5811×10^{-3}
0.184 59 (1.200×10^{15})	0.011 36	0.013 77	0.014 13
0.208 65 (1.533×10^{15})	0.021 80	0.025 84	0.026 46
0.230 22 (1.867×10^{15})	0.032 91	0.038 28	0.039 05
0.249 93 (2.200×10^{15})	0.043 38	0.049 56	0.050 34
0.268 20 (2.533×10^{15})	0.052 54	0.058 96	0.059 69
0.285 30 (2.867×10^{15})	0.060 22	0.066 45	0.067 10
0.301 43 (3.200×10^{15})	0.066 51	0.072 31	0.072 90
0.315 24 (3.500×10^{15})	0.071 17	0.076 50	0.077 05
0.337 01 (4.000×10^{15})	0.077 33	0.081 92	0.082 42
0.357 45 (4.500×10^{15})	0.082 09	0.086 07	0.086 54
0.376 78 (5.000×10^{15})	0.085 94	0.089 50	0.089 91
0.395 17 (5.500×10^{15})	0.089 23	0.092 53	0.092 87

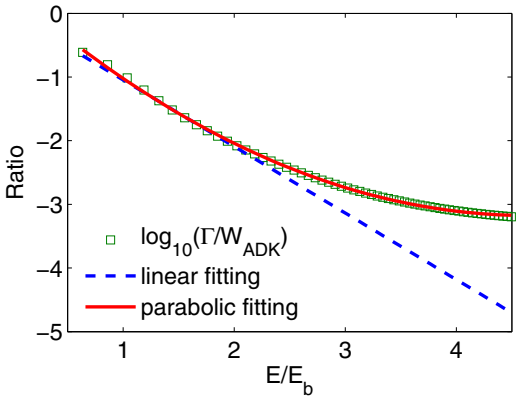

FIG. 1. (Color online) The ratio between the ionization rates obtained with the Schrödinger equation and ADK formula in logarithmic scale (square) and the linear and parabolic fitting using Eq. (8) (dashed and solid line).

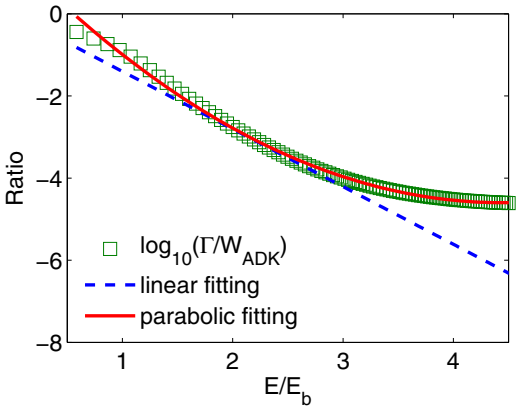

FIG. 2. (Color online) Same as Fig. 1, but the target is Ar^+.

C. Comparison of the SAE models: static ionization rate

Next the static ionization rate was calculated with the above GSZ, Muller, and Tong-Lin SAE models, respectively. We assume that a dc electric field is applied and Ar is considered. The amplitude of the electric field varies from 0.053 to 0.32 a.u., which corresponds to intensities from 1.0×10^{14} to 3.5×10^{15} W/cm^2. The half static ionization rates ($\Gamma/2$) are shown in Table IX.

One can see that the ionization rates obtained with GSZ and Muller SAE models are very close. The ionization rate obtained with Tong and Lin's SAE model is slightly higher, but the relative deviation is very small. When the intensity is lower than 1×10^{15} W/cm^2, the relative deviation is about 10%. It gradually decreases to 5% at 2×10^{15} W/cm^2 and finally decreases to 1% at 3×10^{15} W/cm^2.

We also checked the static ionization rates of Ar^+, which are shown in Table X. In this case, Tong and Lin's and Muller's models give very close results. The GSZ model slightly underestimates the ionization rate compared with Tong and Lin's and Muller's models, but the difference is also small. One can say that the above three SAE models agree well with each other. He, Ne, and other atoms are also tested, and similar results are obtained. It is noted that the multielectron effects beyond the SAE approximation on ionization have not been included in our calculation. At relative high-field strength, the amplitude of population of the ionic state is disturbed by the external laser field [33], which is responsible for the influence of the multielectron on ionization. On the other hand, the electron-electron and electron-ion interactions play a more important role at low-field strength [34] due to the relatively strong Coulomb interaction.

D. Comparison of the ionization rate: ADK, WFAT, Tong-Lin, and Schrödinger simulation

Since the ADK and WFAT ionization formulas work only in the tunneling regime, we therefore first check the performance of Tong and Lin's ionization formula in the over-barrier regime. We define the logarithmic ratio between the quantum simulation results and ADK ionization rates, i.e., $R = \log_{10}(\Gamma/W_{\rm ADK})$. In Fig. 1, R is plotted as a function of laser field strength for Ar in units of E_b. One can clearly see that R decreases almost linearly with the laser amplitude when $E/E_b < 2$. However, in the region of $E/E_b > 2$, R deceases more slowly and gradually departs from its linear fitting (see the dashed line in Fig. 1). That is why Tong and Lin's formula fails in the deep over-barrier region. In this situation, a parabolic fitting is required, which is termed a modified empirical formula. The ionization rate can be corrected by

$$W_M(E) = \exp\left[-\left(a_1\frac{E^2}{E_b^2} + a_2\frac{E}{E_b} + a_3\right)\right] W_{\rm ADK}(E). \quad (8)$$

Using the fitting parameters shown in Table XI, the parabolic ionization curve (see the solid line in Fig. 1) is consistent with the quantum result. For other atoms and ions, such as Ar^+ (see Fig. 2), He, Ne, Kr, and Xe, a good agreement with the exact result is also achieved, and the required fitting parameters are summarized in Table XI.

To get a deep insight into the ADK [$W_{\rm ADK}$, Eq. (1)], WFAT [$W_{\rm WFAT}$, Eq. (2)], Tong-Lin [$W_{\rm TL}$, Eq. (3)], and modified empirical ionization formulas [W_M, Eq. (8)] in the over-barrier regime, we compared these formulas with the quantum simulation results by solving the Schrödinger equation (denoted as Γ). Since the SAE potentials in Secs. II B and II C are consistent for quantum simulation, only the

TABLE XI. Parameters for the modified empirical formula.

Parameter	H	He	Ne	Ar	Kr	Xe	Ar^+
a_1	0.117 14	0.135 50	0.100 61	0.161 78	0.146 40	0.210 80	0.304 41
a_2	−0.909 33	−0.862 10	−1.048 32	−1.504 41	−1.365 33	−1.884 82	−2.704 61
a_3	−0.060 34	0.021 562	−0.075 42	0.321 27	0.020 55	0.574 281	1.408 21

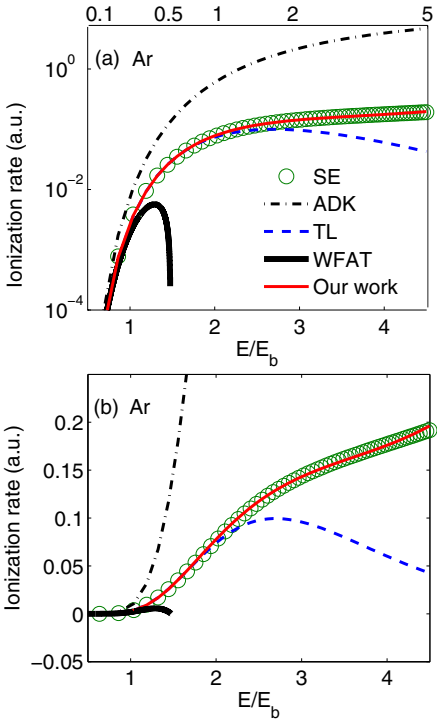

FIG. 3. (Color online) The ionization rates obtained with the Schrödinger equation, ADK [Eq. (1)] formula, WFAT [Eq. (2)] formula, Tong and Lin's formula [Eq. (3)], and modified empirical formula [Eq. (8)] in (a) logarithmic scale and (b) linear scale. The upper axis shows the corresponding laser intensity in units of 1×10^{15} W/cm^2.

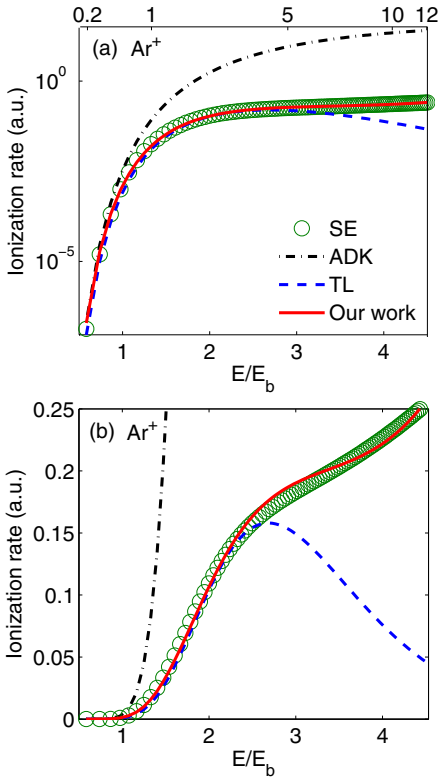

FIG. 4. (Color online) Same as Fig. 3, but the target is Ar^+.

Tong-Lin SAE potentials are used for He, Ne, Ar, Xe, and Ar^+ and the GSZ potential is used for Kr.

Figures 3(a) and 3(b) show the ionization rates calculated with the ADK (dash-dotted line) formula, first-order WFAT (thick solid line), Tong and Lin's (dashed line) formula, the modified empirical formula (thin solid line), and the Schrödinger equation (circles) in logarithmic scale and linear scale for Ar, respectively. Compared with the quantum simulation result, the ADK formula significantly overestimates the ionization rate from the deep tunneling to over-barrier regime. Using the first-order WFAT, the calculated ionization rate agrees quite well with the quantum one when $E < E_b$. Tong and Lin's formula further extends the region of applicability of ionization calculation to a field strength up to $2E_b$. However,Tong and Lin's formula underestimates the ionization rate in the deep over-barrier region with a laser field strength higher than $2E_b$. For the modified empirical formula, the obtained ionization rate is consistent with the exact quantum result in the whole region from $E/E_b = 0.5$ to 4.5.

The same calculation procedure has been performed for other ions and atoms. Figure 4 shows one example of Ar^+. A similar trend can be observed: Tong and Lin's formula works very well if $E/E_b < 2$ but underestimates the ionization rate in the deep over-barrier regime. Therefore, we suggest the modified empirical formula [Eq. (8)] instead of Tong and Lin's formula [Eq. (3)].

To check the performances of Eqs. (3) and (8), we introduce the relative error defined by

$$\text{Error} = \frac{W - \Gamma}{\Gamma}. \tag{9}$$

Figure 5 shows the relative error between the ionization rate calculated with the Schrödinger equation and those calculated with Eqs. (3) and (8) for different atoms. The ionization rates calculated with the modified empirical formula [Eq. (8)] agree very well with the quantum simulation results from $E/E_b = 0.5$ to 4.5. The relative errors are less than 0.2 for He, Ne, Ar, Kr, and Xe atoms. For the Ar^+ ion, the relative errors are less than 0.15 if $0.7 < E/E_b < 4.5$, but slight larger if $E/E_b < 0.7$. These results give evidence that the modified empirical formula has enough accuracy for calculating ionization rates, especially in the deep over-barrier regime. On the other hand, Tong and Lin's formula [Eq. (3)] is also valid with laser field strength up to $E/E_b = 2$ while it has large relative errors in the deep over-barrier regime due to the rapid increase with the laser intensity. For the He atom, the relative error is 0.02 at $E/E_b = 1.5$, but increases to 0.29 at $E/E_b = 2.5$ and 0.74 at $E/E_b = 4.5$.

In practice, the ionization rate with the survival probability becomes important when the electric-field strength is high enough. Since the use of few-cycle laser pulses can avoid significant ionization of the atom by the leading edge of the pulse, we therefore evaluate the total ionization probability of the Ar atom in a 2-fs pulsed laser with varying peak intensities. The 2-fs laser pulse can be experimentally achieved by synthesizing a 1.5-octave three-channel optical field spanning the infrared, visible, and ultraviolet frequency regimes [35].

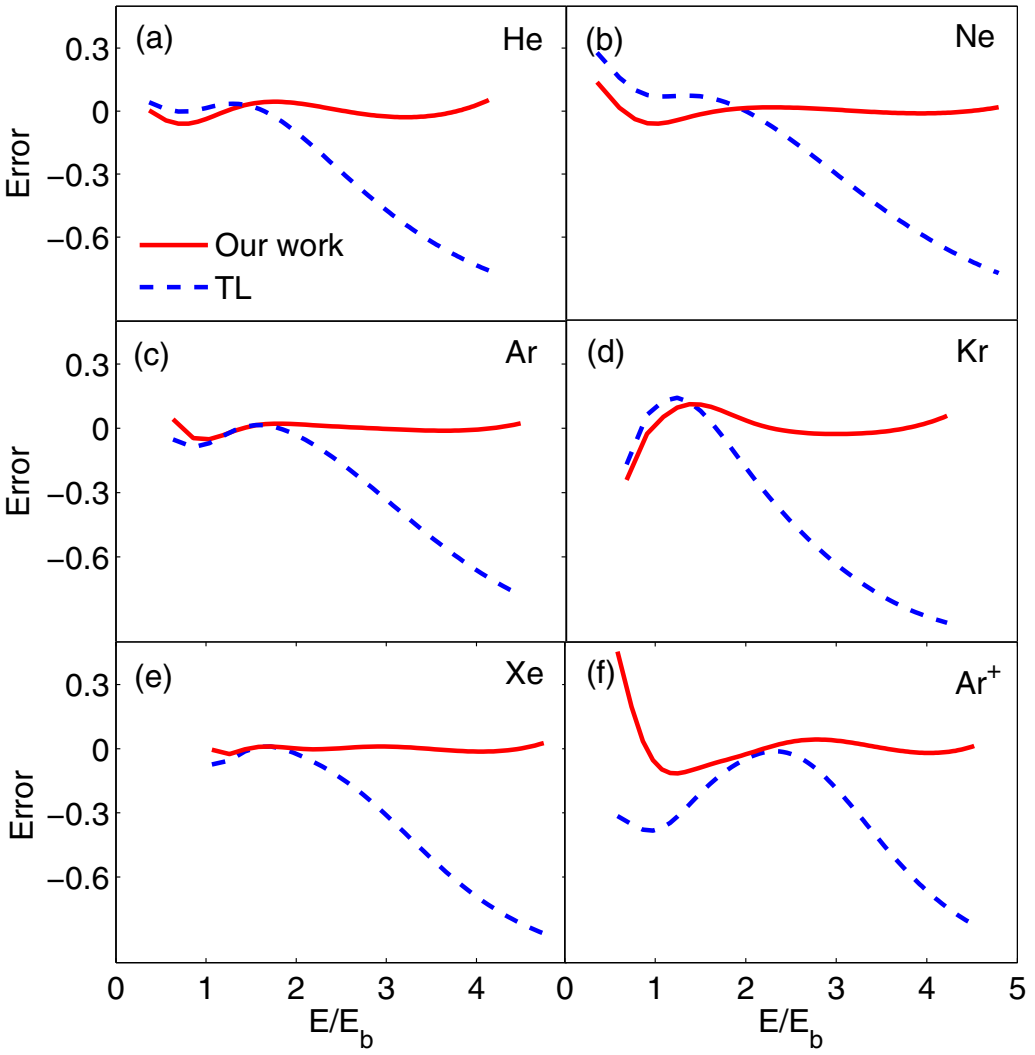

FIG. 5. (Color online) Relative error between the ionization rates calculated with the Schrödinger equation and those calculated with Eqs. (3) and (8). The targets are He, Ne, Ar, Kr, Xe, and Ar^+, respectively.

By using the ionization rates shown in Eqs. (3) and (8), the ionization probabilities at the end of the pulse are calculated as

$$P = 1 - \exp^{\int_{-\infty}^{+\infty} W[E(t)]dt}. \tag{10}$$

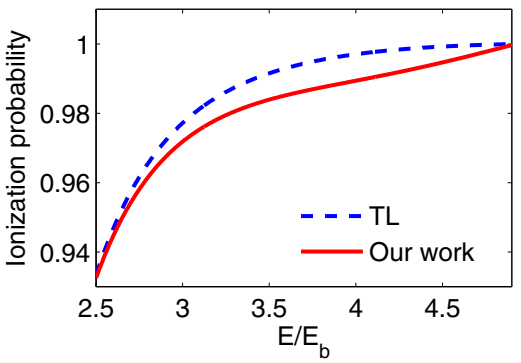

FIG. 6. (Color online) Ionization probabilities of the Ar atom in the 2-fs laser pulses with varying peak intensities.

From Fig. 6, it is clear that the probability curve calculated using Tong and Lin's rate deviates from the one obtained with our modified empirical ionization rate. The probability calculated from the Tong-Lin model predicts larger ionization probability at higher intensities. Based on the two curves in Fig. 6 the saturation field strength calculated from the Tong-Lin model is $3.47E_b$ (2.98×10^{15} W/cm^2) while from the modified empirical model it is $4.06E_b$ (4.08×10^{15} W/cm^2). Here, the saturation field strength is defined when the total ionization probability is 99%.

III. SUMMARY

In summary, a modified empirical formula for over-barrier ionization is proposed. By solving the Schrödinger equation, the validity of this modified empirical formula has been confirmed for a field strength covering the tunneling to deep over-barrier regime, and the upper limit of applicable field strength for this formula is determined to be $4.5E_b$. We believe that the upper limit of $4.5E_b$ for this formula is strong enough for most experiments in strong-field physics. For instance,

$4.5E_b$ corresponds to the laser intensities of $5 \times 10^{15}\,\mathrm{W/cm^2}$ for Ar and most investigations on Ar using laser intensities lower than these values. Moreover, the relative error of the modified empirical formula rapidly increases if $E > 4.5E_b$, and in that case even more complicated parameters may be required for fitting the quantum simulation results.

ACKNOWLEDGMENTS

This work was supported by the National Natural Science Foundation of China under Grants No. 11204095, No. 61275126, No. 11234004, and No. 61475055 and by the 973 Program of China under Grant No. 2011CB808103.

[1] P. Agostini, F. Fabre, G. Mainfray, G. Petite, and N. K. Rahman, Phys. Rev. Lett. **42**, 1127 (1979).
[2] A. McPherson, G. Gibson, H. Jara, U. Johann, T. S. Luk, I. A. McIntyre, K. Boyer, and C. K. Rhodes, J. Opt. Soc. Am. B **4**, 595 (1987).
[3] P. Lambropoulos, X. Tang, P. Agostini, G. Petite, and A. L'Huillier, Phys. Rev. A **38**, 6165 (1988).
[4] M. V. Ammosov, N. B. Delone, and V. P. Kraĭnov, Zh. Éksp. Teor. Fiz. **91**, 2008 (1986) [Sov. Phys. JETP **64**, 1191 (1986)].
[5] A. M. Perelomov, V. S. Popov, and M. V. Terent'ev, Zh. Eksp. Teor. Fiz. **50**, 1393 (1966) [Sov. Phys. JETP **23**, 924 (1966)].
[6] O. I. Tolstikhin, T. Morishita, and L. B. Madsen, Phys. Rev. A **84**, 053423 (2011).
[7] L. B. Madsen, O. I. Tolstikhin, and T. Morishita, Phys. Rev. A **85**, 053404 (2012).
[8] L. B. Madsen, F. Jensen, O. I. Tolstikhin, and T. Morishita, Phys. Rev. A **87**, 013406 (2013).
[9] V. H. Trinh, O. I. Tolstikhin, L. B. Madsen, and T. Morishita, Phys. Rev. A **87**, 043426 (2013).
[10] O. I. Tolstikhin, L. B. Madsen, and T. Morishita, Phys. Rev. A **89**, 013421 (2014).
[11] L. B. Madsen, F. Jensen, O. I. Tolstikhin, and T. Morishita, Phys. Rev. A **89**, 033412 (2014).
[12] A. Scrinzi, M. Geissler, and T. Brabec, Phys. Rev. Lett. **83**, 706 (1999).
[13] X. M. Tong and C. D. Lin, J. Phys. B **38**, 2593 (2005).
[14] A. N. Pfeiffer, C. Cirelli, M. Smolarski, R. Dorner, and U. Keller, Nat. Phys. **7**, 428 (2011).
[15] J. S. Parker, K. J. Meharg, G. A. McKenna, and K. T. Taylor, J. Phys. B **40**, 1729 (2007).
[16] J. L. Hansen, L. Holmegaard, L. Kalhøj, S. L. Kragh, H. Stapelfeldt, F. Filsinger, G. Meijer, J. Küpper, D. Dimitrovski, M. Abu-samha, C. P. J. Martiny, and L. B. Madsen, Phys. Rev. A **83**, 023406 (2011).
[17] D. B. Milošević, W. Becker, M. Okunishi, G. Prümper, K. Shimada, and K. Ueda, J. Phys. B **43**, 015401 (2010).
[18] K. Yamakawa, M. Aoyama, S. Matsuoka, T. Kase, Y. Akahane, and H. Takuma, Opt. Lett. **23**, 1468 (1998).
[19] A. L. Cavalieri, E. Goulielmakis, B. Horvath, W. Helml, M. Schultze, M. Fiess, V. Pervak, L. Veisz, V. S. Yakovlev, M. Uiberacker, A. Apolonski, F. Krausz, and R. Kienberger, New J. Phys. **9**, 242 (2007).
[20] E. J. Takahashi, T. Kanai, Y. Nabekawa, and K. Midorikawa, Appl. Phys. Lett. **93**, 041111 (2008).
[21] Y. Deng, A. Schwarz, H. Fattahi, M. Ueffing, X. Gu, M. Ossiander, T. Metzger, V. Pervak, H. Ishizuki, T. Taira, T. Kobayashi, G. Marcus, F. Krausz, R. Kienberger, and N. Karpowicz, Opt. Lett. **37**, 4973 (2012).
[22] Q. Zhang, E. J. Takahashi, O. D. Mücke, P. Lu, and K. Midorikawa, Opt. Express **19**, 7190 (2011); Z. Hong, Q. Zhang, and P. Lu, *ibid.* **21**, 9491 (2013); **22**, 5544 (2014).
[23] L. He, Y. Li, Q. Zhang, and P. Lu, Opt. Express **21**, 2683 (2013); Q. Zhang, P. Lu, W. Hong, Q. Liao, and S. Wang, Phys. Rev. A **80**, 033405 (2009).
[24] C. M. Maharjan, A. S. Alnaser, X. M. Tong, B. Ulrich, P. Ranitovic, S. Ghimire, Z. Chang, I. V. Litvinyuk, and C. L. Cocke, Phys. Rev. A **72**, 041403(R) (2005).
[25] Y. Zhou, C. Huang, Q. Liao, and P. Lu, Phys. Rev. Lett. **109**, 053004 (2012); Y. Zhou, Q. Zhang, C. Huang, and P. Lu, Phys. Rev. A **86**, 043427 (2012); Q. Liao, Y. Zhou, C. Huang, and P. Lu, New J. Phys. **14**, 013001 (2012).
[26] P. Lan, Y. Zhou, A. N. Pfeiffer, Q. Zhang, P. Lu, and K. Midorikawa, Phys. Rev. A **89**, 033424 (2014).
[27] P. B. Corkum, Phys. Rev. Lett. **71**, 1994 (1993).
[28] A. Maquet, S. I. Chu, and W. P. Reinhardt, Phys. Rev. A **27**, 2946 (1983).
[29] C. J. Lai, G. Cirmi, K. H. Hong, J. Moses, S. W. Huang, E. Granados, P. Keathley, S. Bhardwaj, and F. X. Kartner, Phys. Rev. Lett. **111**, 073901 (2013).
[30] A. E. S. Green, D. L. Sellin, and A. S. Zachor, Phys. Rev. **184**, 1 (1969); P. S. Ganas and A. E. S. Green, Phys. Rev. A **4**, 182 (1971).
[31] H. G. Muller, Phys. Rev. A **60**, 1341 (1999).
[32] The atomic spectra includes the multielectron effect. The configuration of the multielectron state could be very complex. We show only one or two values for each eigenstate.
[33] O. Smirnova, Y. Mairesse, S. Patchkovskii, N. Dudovich, D. Villeneuve, P. Corkum, and M. Yu. Ivanov, Nature (London) **460**, 972 (2009).
[34] A. N. Pfeiffer, C. Cirelli, M. Smolarski, X. Wang, J. H. Eberly, R. Döner, and U. Keller, New J. Phys. **13**, 093008 (2011).
[35] A. Wirth, M. T. Hassan, I. Grguraš, J. Gagnon, A. Moulet, T. T. Luu, S. Pabst, R. Santra, Z. A. Alahmed, A. M. Azzeer, V. S. Yakovlev, V. Pervak, F. Krausz, and E. Goulielmakis, Science **334**, 195 (2011).